Published OnlineFirst January 9, 2020; DOI: 10.1158/2159-8290.CD-19-0400

RESEARCH BRIEF

Circadian Regulator CLOCK Recruits Immune-Suppressive Microglia into the GBM Tumor Microenvironment

Peiwen Chen[1], Wen-Hao Hsu[1], Andrew Chang[1], Zhi Tan[1], Zhengdao Lan[1], Ashley Zhou[1], Denise J. Spring[1], Frederick F. Lang[2], Y. Alan Wang[1], and Ronald A. DePinho[1]

ABSTRACT Glioblastoma (GBM) is a lethal brain tumor containing a subpopulation of glioma stem cells (GSC). Pan-cancer analyses have revealed that stemness of cancer cells correlates positively with immunosuppressive pathways in many solid tumors, including GBM, prompting us to conduct a gain-of-function screen of epigenetic regulators that may influence GSC self-renewal and tumor immunity. The circadian regulator *CLOCK* emerged as a top hit in enhancing stem-cell self-renewal, which was amplified in about 5% of human GBM cases. CLOCK and its heterodimeric partner BMAL1 enhanced GSC self-renewal and triggered protumor immunity via transcriptional upregulation of OLFML3, a novel chemokine recruiting immune-suppressive microglia into the tumor microenvironment. In GBM models, *CLOCK* or *OLFML3* depletion reduced intratumoral microglia density and extended overall survival. We conclude that the CLOCK–BMAL1 complex contributes to key GBM hallmarks of GSC maintenance and immunosuppression and, together with its downstream target OLFML3, represents new therapeutic targets for this disease.

SIGNIFICANCE: Circadian regulator CLOCK drives GSC self-renewal and metabolism and promotes microglia infiltration through direct regulation of a novel microglia-attracting chemokine, OLFML3. CLOCK and/or OLFML3 may represent novel therapeutic targets for GBM.

INTRODUCTION

Glioblastoma (GBM) is the most aggressive and lethal form of adult brain cancer, for which current standard of care offers minimal clinical benefit (1). Extensive genomic profiling has identified key alterations of distinct signaling pathways in GBM, including the RTK–RAS–PI3K–PTEN, RB–CDKN2A, and TP53–ARF–MDM2 pathways (2–5). Efforts to target these altered signaling pathways, for example, EGFR or PI3K inhibition, have yielded minimal impact on outcomes of patients with GBM (6–9). Although these genetic alterations affect many intrinsic aspects of cancer cell biology, there is a growing recognition that these alterations also promote the expression of paracrine factors regulating the recruitment and activation of

[1]Department of Cancer Biology, The University of Texas MD Anderson Cancer Center, Houston, Texas. [2]Department of Neurosurgery and Brain Tumor Center, The University of Texas MD Anderson Cancer Center, Houston, Texas.

Note: Supplementary data for this article are available at Cancer Discovery Online (http://cancerdiscovery.aacrjournals.org/).

Corresponding Authors: Ronald A. DePinho, The University of Texas MD Anderson Cancer Center, 1881 East Road, Unit 1906, Houston, TX 77030. Phone: 832-751-9756; Fax: 713-745-7167; E-mail: rdepinho@mdanderson.org; and Y. Alan Wang, yalanwang@mdanderson.org

Cancer Discov 2020;10:1–11

doi: 10.1158/2159-8290.CD-19-0400

Published OnlineFirst January 9, 2020; DOI: 10.1158/2159-8290.CD-19-0400

immune-suppressive cells in the tumor microenvironment (TME; refs. 10, 11). In GBM, for example, we demonstrated that *PTEN* deletion/mutation can drive expression of lysyl oxidase (LOX), which promotes infiltration of immunosuppressive tumor-associated macrophages (TAM) that in turn provide growth factor support for glioma cell survival (12). Such studies highlight the opportunities of identifying genetic alterations in glioma cells that establish symbiotic cancer–host interactions including immune suppression mechanisms in the TME.

In addition to the above genetic alterations, dysregulation of epigenetic programs is also known to affect tumor biology on many levels (13–15). In particular, various epigenetic regulators have been shown to play critical roles in the maintenance of glioma stem cells (GSC; such as N^6-mA, EZH2, and DAXX) and in the regulation of tumor immunity (such as histone deacetylases; refs. 16, 17). These regulatory factors gain added significance as GSCs are critical to both tumor maintenance and therapeutic resistance in GBM (16). Moreover, pan-cancer computational analyses have demonstrated a positive correlation between stemness and immune signatures (18). Together, these insights prompted us to conduct a gain-of-function screen of known epigenetic regulators that may dually enhance GSC self-renewal and promote an immune-suppressive TME. In this screen, the circadian regulator *CLOCK* emerged as the top hit.

The circadian rhythm serves as an important regulatory system maintaining homeostasis in normal cells and tissues (19, 20) and has been shown to play a pivotal role in cancer-relevant processes such as cell proliferation and survival, DNA repair, metabolism, and inflammation (19–21). CLOCK and BMAL1 (also known as ARNTL) are two key transcription factors of the circadian machinery, which constitute a heterodimeric complex (22). This complex can activate the expression of the *PER* and *CRY* genes, which ultimately forms a negative feedback loop to inhibit the activity of the CLOCK–BMAL1 complex (22).

There is an increasing recognition that the impact of CLOCK and BMAL1 on cancer pathogenesis is highly context- and disease-dependent (21). For instance, CLOCK or BMAL1 provides tumor suppressor–like functions in prostate, breast, ovarian, and pancreatic cancers, but exhibits tumor-promoting roles in colorectal cancer and acute myeloid leukemia (21, 23). In GBM, CLOCK or BMAL1 is a tumor-promoting factor that regulates glioma-cell proliferation and migration via regulation of the NFκB pathway (24) and can support GSC function via regulation of anabolic metabolism (25). Here, we elucidate a novel function for CLOCK in supporting an immune-suppressive TME via its upregulation of OLFML3, a novel and potent chemoattractant of immune-suppressive microglia. Clinicopathologic correlations in human GBM point to CLOCK and OLFML3 as potential therapeutic targets for GBM.

RESULTS

CLOCK Promotes GSC Self-Renewal and Is Amplified in Human GBM

Employing previously characterized human neural stem cells (hNSC; ref. 26), a gain-of-function screen revealed that 31 of 284 epigenetic regulators could enhance hNSC self-renewal activity (Fig. 1A). CLOCK exhibited the highest self-renewal activity which was comparable with the positive control myr-AKT, and CLOCK overexpression was confirmed by immunoblot analysis (Supplementary Fig. S1A). Examination of The Cancer Genome Atlas (TCGA) GBM datasets revealed that *CLOCK*, but not genes encoding other epigenetic factors, is amplified in approximately 5% of GBM cases (Fig. 1B; Supplementary Fig. S1B) and 2.8% of low-grade glioma cases (Fig. 1C). Furthermore, increased gene copy number correlated positively with increased *CLOCK* mRNA levels (Fig. 1D). To further confirm the relevance of CLOCK in promoting GSC self-renewal and maintenance, we conducted shRNA-mediated depletion studies in human GSCs having relatively high CLOCK expression, such as GSC20, GSC167, and GSC272 (Supplementary Fig. S1C). Constitutive *CLOCK* depletion was associated with impaired self-renewal of GSC20 and GSC167 (Supplementary Fig. S1D and S1E), and an inducible shRNA knockdown system, termed ish*CLOCK*, reduced self-renewal in GSC272 and GSC20 (Fig. 1E; Supplementary Fig. S1F and S1G). Finally, we conducted shRNA-mediated *CLOCK* depletion in mouse QPP7 GSC having relatively high CLOCK expression (Supplementary Fig. S1C), and found that *CLOCK* depletion impaired QPP7 self-renewal, which can be rescued by reexpression of shRNA-resistant *CLOCK* cDNA (Supplementary Fig. S1H).

CLOCK heterodimerizes with BMAL1 to form a transcription factor complex that regulates core circadian clock genes (22). Within the heterodimer, depletion of one partner induces degradation of the other component (27). Indeed, we found that shRNA-mediated depletion of *BMAL1* reduced CLOCK expression (Fig. 1F) and impaired self-renewal activity of GSC20 and GSC272 (Fig. 1G). SR9009 is an agonist of the nuclear receptors REV–ERBs, which function as direct negative regulators of the CLOCK–BMAL1 complex (28). SR9009 treatment inhibited the self-renewal ability of GSC20 and GSC272 (Fig. 1H), reinforcing the role of CLOCK/BMAL1 in promotion of GSC self-renewal.

Figure 1. CLOCK is amplified in GBM and regulates GSC self-renewal. **A,** Soft-agar colony formation of hNSCs overexpressing indicated epigenetic genes. $n = 3$ biological replicates. **B,** Genomic alterations of *CLOCK* and other epigenetic regulators (*CHD2, KMT5C, SSRP1, FBXL19, JMJD8, PCMT1, NAP1L2, JMJD7*, and *ACTR6*) in TCGA GBM database (provisional dataset; $n = 528$). **C,** Genomic alteration frequency of *CLOCK* in TCGA GBM datasets, GBM–LGG merged dataset and LGG datasets. **D,** *CLOCK* copy number is significantly correlated with *CLOCK* mRNA expression in TCGA GBM patients ($n = 508$). ++, high level of amplification; +, gain; Neutral, no change; ±, homozygous deletion. **, $P < 0.01$; ***, $P < 0.001$. **E,** Conditional depletion of *CLOCK* suppresses GBM tumorsphere formation. Representative images (left) and quantification (right) of tumorspheres in GSC272 cells expressing ish*CLOCK* or ishControl. Scale bar, 100 μm. $n = 3$ biological replicates; ***, $P < 0.001$. **F,** Immunoblots for CLOCK and BMAL1 in cell lysates of GSC272 and GSC20 expressing shRNA control (shC) or *BMAL1* shRNAs. **G,** *BMAL1* depletion impairs GSC tumorsphere formation. Representative images (left) and quantification (right) of tumorspheres in GSC20 and GSC 272 expressing two independent *BMAL1* shRNAs or shControl. Scale bar, 100 μm. $n = 4$ biological replicates; ***, $P < 0.001$. **H,** SR9009 treatment impairs GSC tumorsphere formation. Representative images (left) and quantification (right) of tumorspheres in GSC20 and GSC272 treated with SR9009 at indicated concentrations. Scale bar, 100 μm. $n = 4$ biological replicates; ***, $P < 0.001$.

Published OnlineFirst January 9, 2020; DOI: 10.1158/2159-8290.CD-19-0400

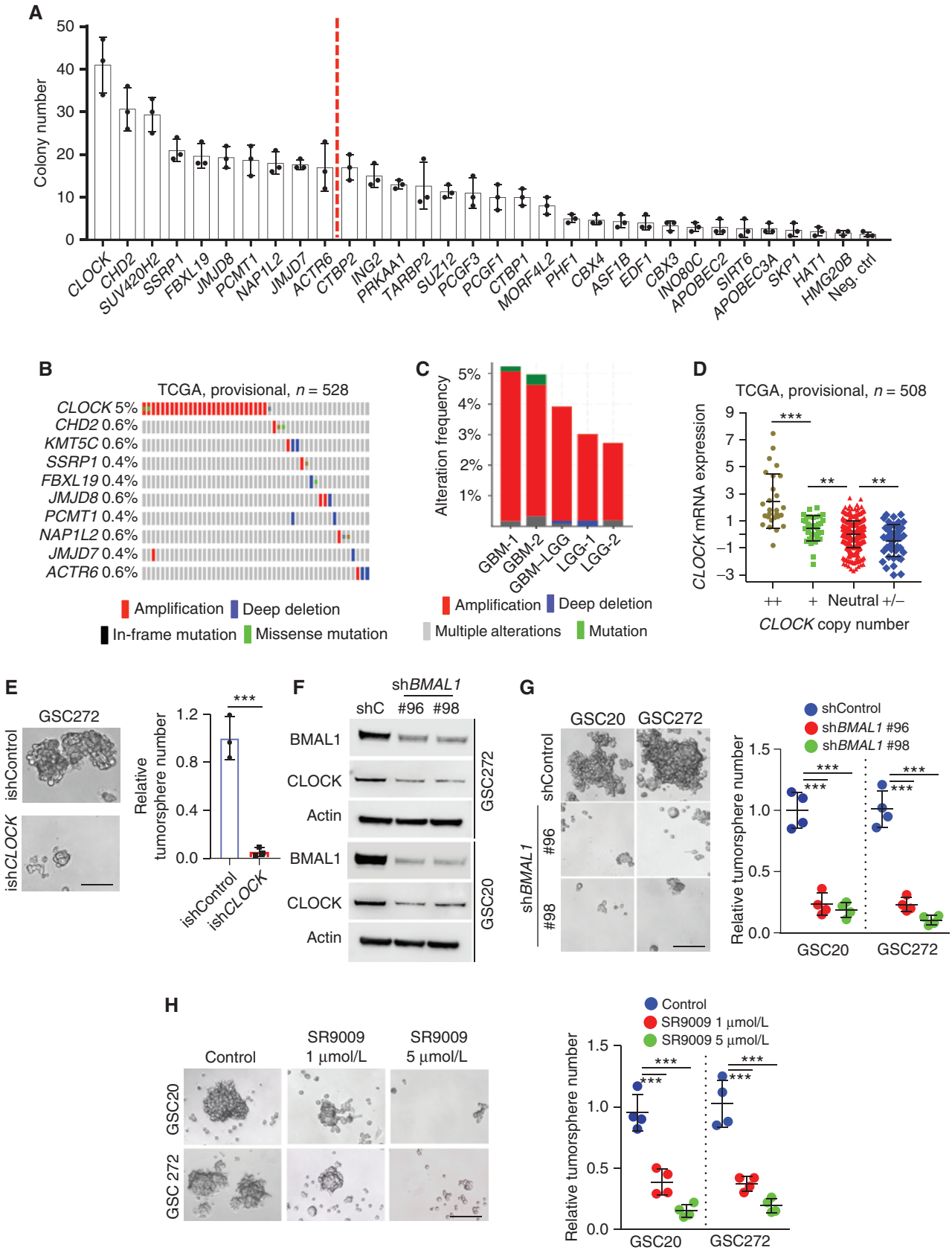

Published OnlineFirst January 9, 2020; DOI: 10.1158/2159-8290.CD-19-0400

To determine the molecular basis of CLOCK's support of GSC self-renewal, gene-expression profiling and Gene Set Enrichment Analysis (GSEA) were compared in GSC272 with ish*CLOCK* versus ishControl. The major pathways affected were related to metabolism, including fatty-acid (FA) metabolism and glycolysis (Supplementary Fig. S2A), which aligns well with previous work showing that FA and glucose metabolism play critical roles in the maintenance of GSC self-renewal (25). Specifically, *CLOCK* depletion resulted in reduced expression of key glycolysis and tricarboxylic acid enzymes such as PGM1, HK2, LDHA, ACO2, SUCLA2, OGDH, and CS as well as FA enzymes such as ACACA, HSD17B, RPP14, ACAT1, and HADH (with PGM1 and ACACA showing the most dramatic reduction; Supplementary Fig. S2B and S2C). Treatment with a PGM1 inhibitor (lithium) or ACACA inhibitor (CP-640186) significantly impaired GSC272 self-renewal, and CLOCK-induced upregulation of self-renewal in GSC17 was blocked by inhibition of PGM1 or ACACA (Supplementary Fig. S2D and S2E). These findings are consistent with previous reports establishing CLOCK as a major regulator of metabolic pathways shown to be critical in supporting GSC self-renewal (25).

CLOCK Promotes Microglia Infiltration in GBM

In addition to therapeutic resistance, high stemness of cancer cells has been shown to correlate positively with immunosuppressive pathways in 21 types of solid tumors, including GBM (18). Indeed, in *CLOCK*-depleted GSCs, GSEA revealed prominent representation of immune-suppressive signatures, including IFNγ/α response, TNFα/NFκB signaling, and inflammatory response (Fig. 2A). These immune signatures prompted *in silico* immune-cell auditing of TCGA GBM datasets using validated gene set signatures for 18 types of immune cells (10, 29–31). Analysis of immune-cell signatures showed that high *CLOCK* expression correlated positively with increased microglia and, to a lesser extent, hematopoietic stem cells, and with decreased $CD8^+$ activated T cells and dendritic cells; other immune-cell types were not significantly changed (Fig. 2B; Supplementary Fig. S3A). Correspondingly, using transwell migration assays, conditioned media (CM) from *CLOCK* shRNA knockdown GSC272, GSC20, U87, or QPP7 cells exhibited reduced microglia migration relative to CM from shRNA control cells (Fig. 2C; Supplementary Fig. S3B–S3D). Moreover, the impaired microglia migration in *CLOCK* shRNA knockdown QPP7 cells can be rescued by reexpression of shRNA-resistant *CLOCK* cDNA (Supplementary Fig. S3D). Similarly, CM from sh*BMAL1* GSC20 cells inhibited microglia migration compared with CM from shControl cells (Fig. 2D). Conversely, CM from hNSC and GSC17 with enforced CLOCK expression increased microglia migration relative to controls (Fig. 2E; Supplementary Fig. S3E and S3F). Finally, in human GBM tissue microarrays (TMA), CLOCK and BMAL1 signals showed a strong positive correlation with expression of the microglia markers TMEM119 and CX3CR1 (Fig. 2F and G). Together, these findings point to a potential link between high CLOCK expression and infiltration of immune-suppressive microglia into the GBM TME.

CLOCK-Regulated OLFML3 Promotes Microglia Migration

To identify putative CLOCK-regulated secreted factors governing microglia recruitment, our microarray profiling data were intersected with a secreted protein database (32). Using a ≥4.0-fold change in expression, coupled with qRT-PCR validation, 11 genes tracked positively with *CLOCK* expression including *OLFML3, POSTN, TFPI2, LGMN, ALDH9A1, MCCC1, COL11A1, LYNX1, TFPI, LIPA*, and *RBP4*. *OLFML3* showed the most dramatic decrease in ish*CLOCK* GSC272 cells (Fig. 3A and B). Gene Ontology Enrichment Analysis (GOEA) on the subontology of Biological Process in TCGA patients with GBM showed that *OLFML3, LGMN*, and *LIPA*, but not other factors, correlated with leukocyte migration and chemotaxis (Supplementary Fig. S4). Among these three genes, only *OLFML3* was reduced by *CLOCK* depletion in GSC20 (Supplementary Fig. S5A). Moreover, TCGA GBM bioinformatics analysis demonstrated that the expression of *OLFML3, LGMN*, and *LIPA* correlated positively with microglia markers (CX3CR1 and TMEM119), with *OLFML3* showing the most significant correlation prompting further in-depth analysis (Supplementary Fig. S5B). Further studies using immunoblotting demonstrated that shRNA-mediated depletion of *CLOCK* or *BMAL1* reduced OLFML3 expression in several GSC models, including mouse QPP7 (Fig. 3C) and human GSC20 and GSC272 (Fig. 3D). *CLOCK* depletion–induced decrease of OLFML3 expression in QPP7 cells was rescued by reexpression of shRNA-resistant *CLOCK* cDNA (Supplementary Fig. 5C).

Using transwell migration assays, recombinant OLFML3-supplemented medium dramatically increased microglia migration in a dose-dependent manner, which was comparable with the activity of the prototypical microglial chemokine CCL2 (aka, MCP1; Fig. 3E). Conversely, CM from shRNA-mediated depletion of OLFML3 in GSC272 or U87 cells showed reduced microglia migration (Fig. 3F; Supplementary Fig. S5D and S5E). To assess whether CLOCK and BMAL1 directly regulate *OLFML3* expression, chromatin immunoprecipitation (ChIP)-PCR assays were performed, showing that CLOCK and BMAL1 bound to the *OLFML3* promoter and that this binding was

Figure 2. CLOCK promotes microglia infiltration in GBM. **A,** Transcriptomic profiling in GSC272 cells following *CLOCK* depletion shows top ten enriched hallmark pathways by GSEA. Blue bars indicate the signatures relate to immune response. **B,** GSEA shows the normalized enrichment score (NES) of various types of immune cells in *CLOCK*-high and *CLOCK*-low patients in TCGA GBM provisional dataset ($n = 528$). Microglia are the most enriched immune cells in *CLOCK*-high patients. The lower quartile was set as the cut-off value. Blue bars indicate FDR < 0.25. **C,** CM from *CLOCK*-depleted GSC272 cells shows reduced ability to attract human HMC3 microglia in a transwell assay. Representative images (left) and quantification (right). Scale bar, 200 μm; $n = 3$ biological replicates; **, $P < 0.01$. **D,** CM from *BMAL1*-depleted GSC20 cells shows reduced ability to attract HMC3 microglia in a transwell assay. Representative images (left) and quantification (right). Scale bar, 250 μm; $n = 3$–4 biological replicates; ***, $P < 0.001$. **E,** CM from *CLOCK*-overexpressing (OE) hNSCs and GSC17 promotes HMC3 microglia migration in a transwell assay. $n = 3$ biological replicates; ***, $P < 0.001$. **F,** *CLOCK* and *BMAL1* expression is positively correlated with microglia markers (TMEM119 and CX3CR1) in TCGA and Rembrandt GBM databases. **G,** CLOCK and BMAL1 expression is positively correlated with CX3CR1 and TMEM119 expression in human GBM TMA samples. Left, representative images showing low and high expression levels of CLOCK, BMAL1, CX3CR1, and TMEM119 in human GBM TMA ($n = 35$). Scale bar, 100 μm. Right, quantification data showing strong positive correlations between CLOCK/BMAL1 and CX3CR1/TMEM119 in human GBM TMA. *R* and *P* values are shown.

Published OnlineFirst January 9, 2020; DOI: 10.1158/2159-8290.CD-19-0400

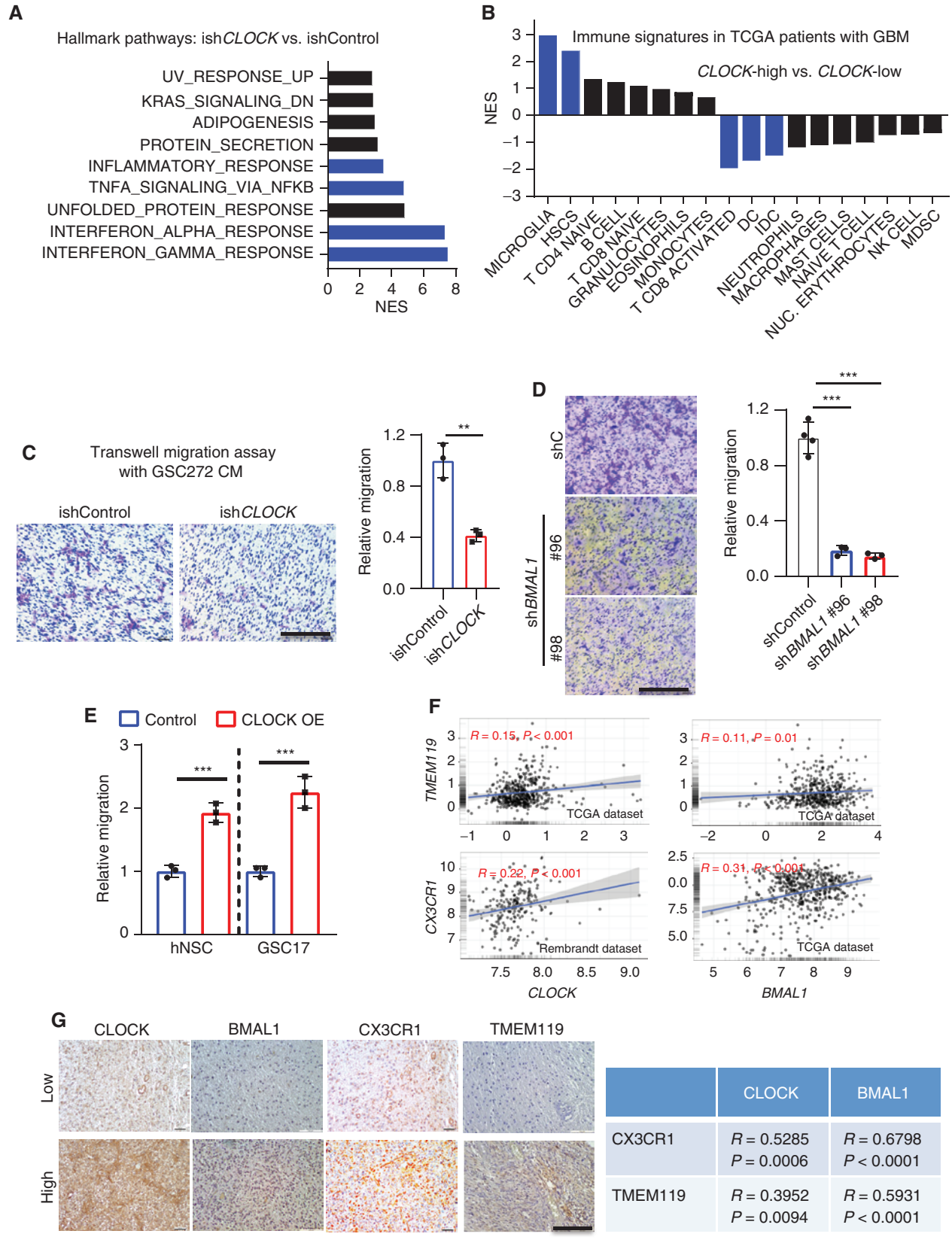

	CLOCK	BMAL1
CX3CR1	$R = 0.5285$ $P = 0.0006$	$R = 0.6798$ $P < 0.0001$
TMEM119	$R = 0.3952$ $P = 0.0094$	$R = 0.5931$ $P < 0.0001$

Published OnlineFirst January 9, 2020; DOI: 10.1158/2159-8290.CD-19-0400

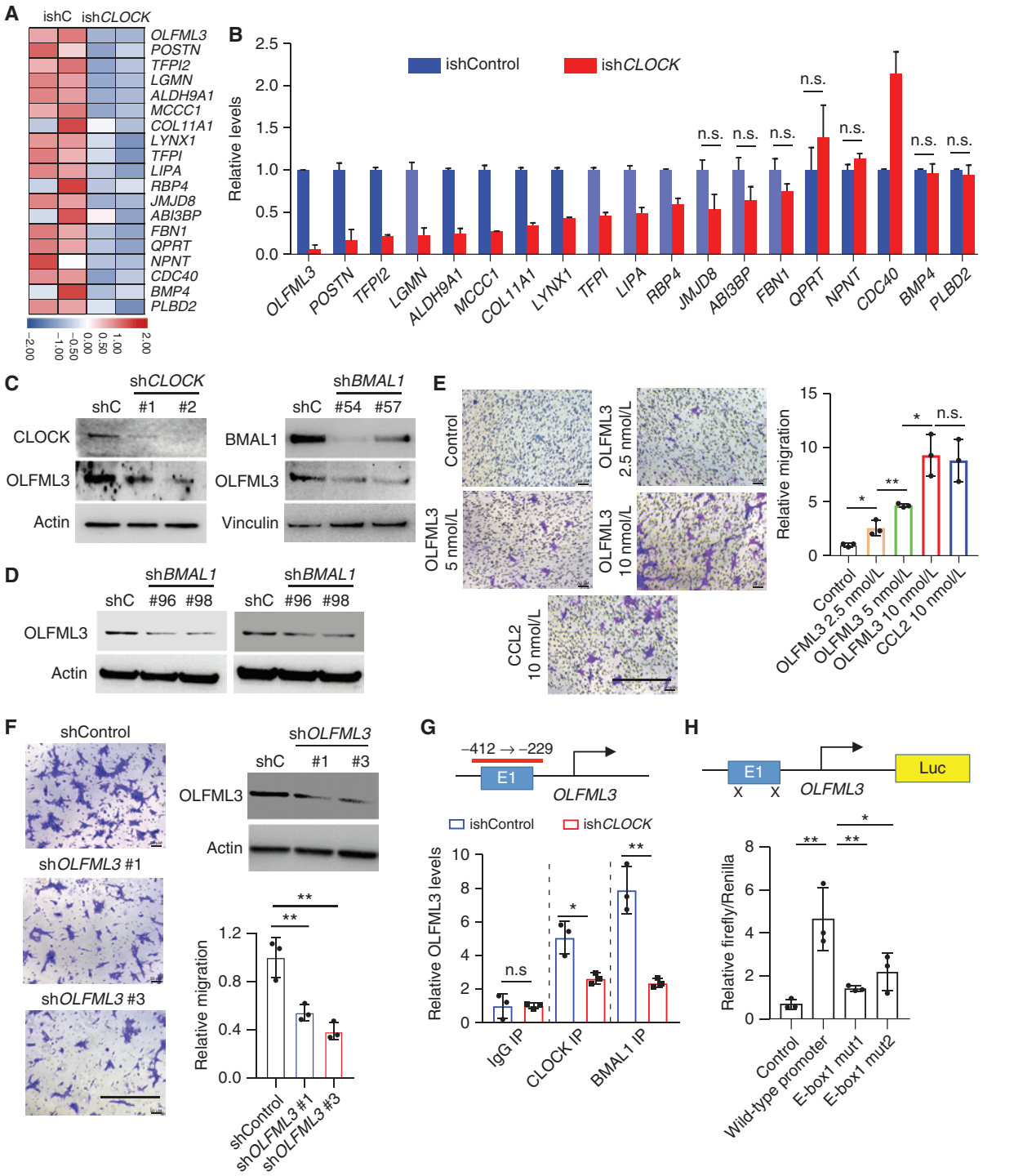

Figure 3. CLOCK-regulated OLFML3 promotes microglia migration. **A,** Heat map representation of the microarray data of ishControl and ish*CLOCK* GSC272 cells shows the most downregulated genes (exhibiting a ≥4-fold change) encoding secreted proteins following *CLOCK* depletion. Red and blue indicate higher and low expression, respectively. **B,** qRT-qPCR validation of downregulated genes as in **A**. n.s., not significant ($P > 0.05$). **C,** Immunoblots for CLOCK and OLFML3 in cell lysates of QPP7 GSCs expressing shRNA control (shC), *CLOCK* shRNAs, or *BMAL1* shRNAs. **D,** Immunoblots for OLFML3 in cell lysates of GSC272 (left) and GSC20 (right) expressing shRNA control (shC) or *BMAL1* shRNAs. **E,** Recombinant OLFML3 protein at indicated concentrations promotes HMC3 microglia migration in transwell assay, and is comparable with positive control CCL2 (10 nmol/L). Representative images (left) and quantification (right). Scale bars, 300 μm; $n = 3$ biological replicates; *, $P < 0.05$; **, $P < 0.01$; n.s., not significant ($P > 0.05$). **F,** *OLFML3*-depleted GSC272 CM impairs HMC3 microglia migration in transwell assay. Representative images (left), shRNA knockdown efficiency and quantification (right). Scale bars, 300 μm; $n = 3$ biological replicates; **, $P < 0.001$. **G,** ChIP-PCR shows that CLOCK and BMAL1 bind to *OLFML3* promoter and that this binding was diminished following *CLOCK* depletion. $n = 3$ biological replicates; *, $P < 0.05$; **, $P < 0.001$; n.s., not significant ($P > 0.05$). **H,** Luciferase (Luc) reporter assay shows that mutations in *OLFML3* promoter E-box sites reduce the transcriptional activity of *CLOCK* for *OLFML3*. $n = 3$ biological replicates; *, $P < 0.05$; **, $P < 0.001$.

Published OnlineFirst January 9, 2020; DOI: 10.1158/2159-8290.CD-19-0400

reduced in *CLOCK*-depleted GSC272 cells (Fig. 3G). Moreover, luciferase reporter assays showed that CLOCK-induced transcriptional activity was abolished by E-box mutations in the *OLFML3* promoter region (Fig. 3H). We conclude that OLFML3 is a novel CLOCK-regulated chemokine with potent microglia recruitment activity.

CLOCK Depletion Inhibits GSC Self-Renewal and Intratumoral Microglia Infiltration and Extends Survival

To further investigate the role of CLOCK in GBM tumor biology, we utilized the ish*CLOCK* system to inducibly deplete *CLOCK* in GSC272 and GSC20 tumors implanted into SCID mice, revealing that *CLOCK* depletion significantly extended survival (Fig. 4A and B; Supplementary Fig. S6A). Using the murine model CT2A, which was isolated from a carcinogen-induced glioma and possesses a GSC-like phenotype (33), depletion of *CLOCK* or *BMAL1* resulted in a significant extension of survival in C57BL/6 mice (Fig. 4C and D). Similarly, pharmacologic inhibition of the CLOCK–BMAL1 complex extended the survival of C57BL/6 mice implanted with CT2A cells (Fig. 4E). On the histologic level, the stem-cell markers OLIG2 and nestin and the proliferation marker Ki-67 were dramatically reduced, whereas apoptosis was increased upon *CLOCK* depletion (Fig. 4F and G; Supplementary Fig. S6B and S6C). In addition, infiltrating microglia were profoundly reduced (10-fold) in the *CLOCK*-depleted tumors (Fig. 4H; Supplementary Fig. S6D). The microglial phenotype, which can be immune-stimulatory (M1) or immunosuppressive (M2; ref. 34), is strongly biased toward the M2 phenotype in both mouse and human GBM tumors (Supplementary Fig. S7A and S7B). M2 microglia were significantly reduced in *CLOCK*-depleted tumors (Supplementary Fig. S7C) and, conversely, the M2 signature correlated positively with high expression levels of *CLOCK* and *BMAL1* in TCGA patients with GBM (Supplementary Fig. S7D and S7E). Because OLFML3 plays a prominent role in microglia migration, we also explored the impact of shRNA-mediated depletion of *OLFML3* on GBM growth, and found that decreased *OLFML3* in the GSC272 model significantly extended survival (Fig. 4I). Together, these *in vivo* results confirm the role of CLOCK in promoting GBM tumor maintenance, which correlates with CLOCK-induced enhancement of stemness, proliferation, and survival, as well as increased recruitment of microglia into the GBM TME.

DISCUSSION

In this study, we uncovered the role and underlying mechanisms of the core circadian regulators CLOCK and BMAL1 in GBM tumor maintenance via its regulation of GSC self-renewal and immunity. We identified OLFML3 as a novel and potent CLOCK-regulated microglia chemoattractant in GBM and demonstrated that OLFML3 depletion can increase survival. The key role of the CLOCK–BMAL1 complex in GBM tumor biology, particularly its regulation of specific metabolic and immunity genes such as *OLFML3*, illuminates potential therapeutic targets governing key cancer hallmarks of stemness and immune suppression.

Circadian rhythm regulators have been extensively studied in model organisms (35) and have been linked to the development of cancers including breast, lung, and colorectal cancers (36, 37). For example, depletion of CLOCK or BMAL1 has been shown to impair leukemia stem-cell proliferation and enhance myeloid differentiation in acute myeloid leukemia (23), as well as suppress glioma cell proliferation and migration (24). Moreover, pharmacologic activation of the circadian clock components REV–ERBs, which repress transcription of *CLOCK* and *BMAL1*, have been shown to impair the growth of multiple cancer types including GBM (28). Specifically, activation of REV–ERBs is selectively lethal to cancer cells by affecting oncogenic drivers (such as *HRAS*, *BRAF*, *PIK3CA*, and others), inducing apoptosis and inhibiting autophagy (28). In this study, we extend the actions of CLOCK in GBM as a promoter of GSC self-renewal, suppressor of antitumor immunity and, consistent with recent reports, regulator of fatty-acid metabolism and glycolysis (25).

A hallmark feature of the GBM TME is an abundance of infiltrating immune cells (38) wherein microglia are known to contribute to an immunosuppressive microenvironment and support GBM progression (39). Here, our findings of CLOCK-regulated microglia recruitment are consistent with previous observations that the immune system can be regulated by circadian components (40) and that dysregulation of the intrinsic circadian clock can alter inflammatory responses (41, 42). In addition, our work also aligns with previous tumor biology findings showing that CLOCK can influence T-cell infiltration in melanoma (43) and that BMAL1 deficiency in endothelial cells impairs the migration of leukocytes in mice (44). Moreover, our mechanistic work reinforces this intimate link by demonstrating the capacity of CLOCK to specifically and directly regulate the chemokine OLFML3, which in turn recruits microglia into the GBM TME.

OLFML3 belongs to the family of olfactomedin domain–containing proteins, which have important roles in tumorigenesis and embryonic patterning (45). Previous work has shown that OLFML3 is a proangiogenic factor in the TME, where it promotes endothelial cell migration and sprouting through activation of the canonical SMAD1/5/8 signaling pathway (45). Along similar lines, it would be useful to determine potential druggable molecular pathways in microglia that are activated by OLFML3, thus expanding therapeutic targets for GBM. Intriguingly, microglia are known to express OLFML3 (46), suggesting that following a CLOCK-directed program of microglia recruitment, microglia themselves could further increase the recruitment of additional microglia through their own secretion of OLFML3 in a feed-forward manner.

TAMs play an important role in GBM tumor biology, prompting assessment of the therapeutic benefit of targeting TAMs in GBM. To date, however, CSF1R inhibitor BLZ945 treatment of mouse GBM models has failed to deplete TAMs and elicited transient antitumor responses (47, 48). Correspondingly, a phase II clinical trial with the CSF1R inhibitor PLX3397 has shown minimal activity in patients with recurrent GBM (49). The basis for these meager responses is not clear, although it is worth noting that 2 of 37 patients with GBM who experienced extended progression-free survival (49) had tumors of the mesenchymal subtype that typically harbors *PTEN* deficiency. Along these lines, our recent studies demonstrated that inhibition of macrophage recruitment by LOX inhibitor specifically impairs *PTEN*-deficient GBM progression, establishing a synthetic lethal interaction between *PTEN*-deficient

Published OnlineFirst January 9, 2020; DOI: 10.1158/2159-8290.CD-19-0400

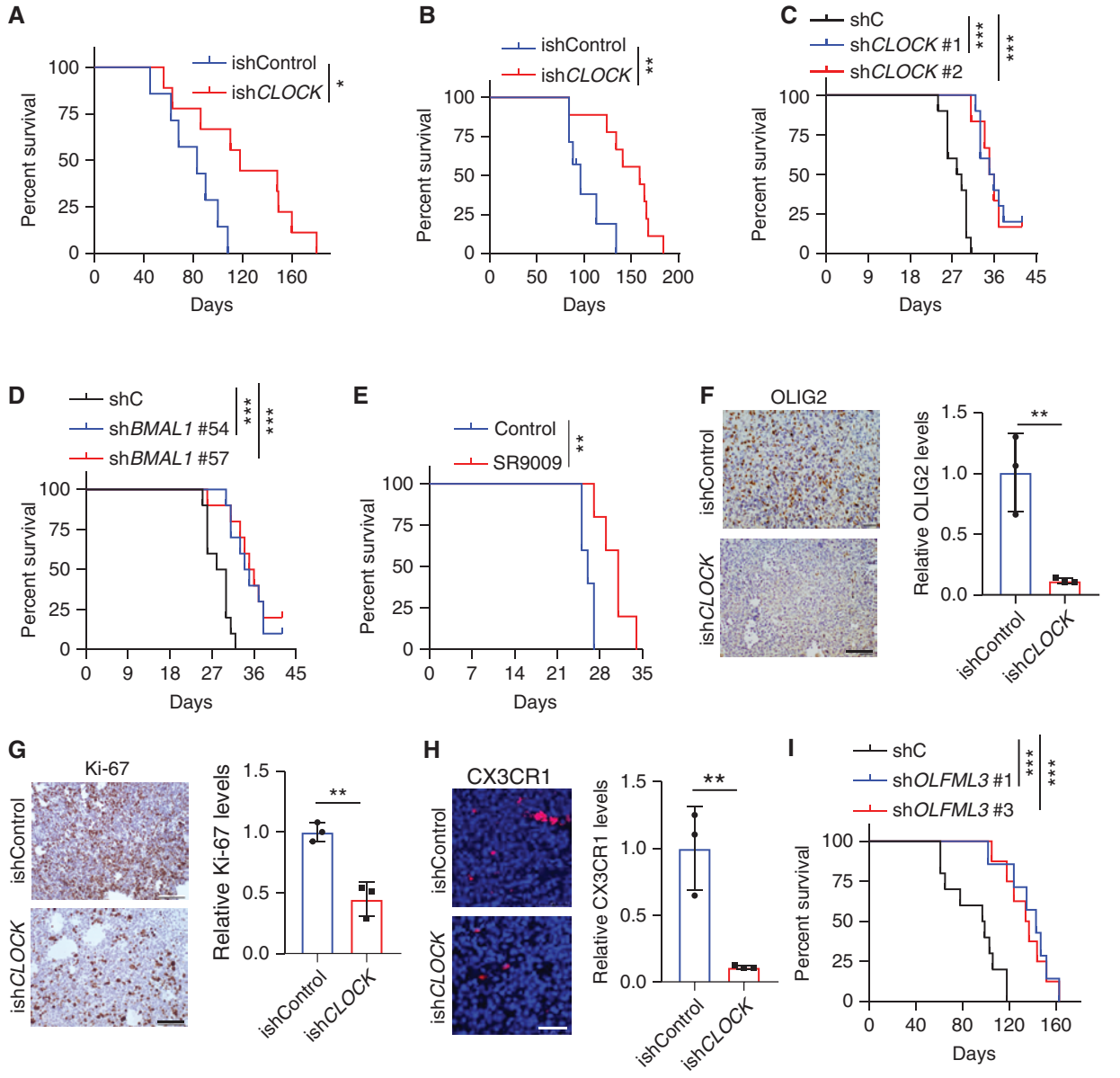

Figure 4. *CLOCK* depletion extends survival, and inhibits GSC self-renewal and microglia infiltration. **A,** Survival curves of SCID mice implanted with ish*CLOCK* and ishControl GSC272 cells (5×10^5 cells). Doxycycline food was provided at day 30 post-orthotopic injection to induce *CLOCK* knockdown *in vivo* ($n = 7$ and 9 mice for ishControl and ish*CLOCK* groups, respectively). *, $P < 0.05$. **B,** Survival curves of SCID mice implanted with ish*CLOCK* and ishControl GSC20 cells (5×10^5 cells). Doxycycline food was provided at day 30 post-orthotopic injection to induce *CLOCK* knockdown *in vivo* ($n = 7$ and 9 mice for ishControl and ish*CLOCK* groups, respectively). **, $P < 0.01$. **C,** Survival curves of C57BL/6 mice implanted with CT2A cells (2×10^4 cells) expressing shRNA control (shC) or *CLOCK* shRNAs ($n = 10$, 10, and 6 mice for shC, sh*CLOCK* #1, and sh*CLOCK* #2 groups, respectively). ***, $P < 0.001$. **D,** Survival curves of C57BL/6 mice implanted with CT2A cells (2×10^4 cells) expressing shRNA control (shC) or *BMAL1* shRNAs ($n = 10$ mice per group). ***, $P < 0.001$. **E,** Survival curves of C57BL/6 mice implanted with CT2A cells (2×10^4 cells). Mice were treated with SR9009 (100 mg/kg, i.p., daily) for 10 days beginning at day 7 post-orthotopic injection ($n = 5$ mice per group). **, $P < 0.01$. **F,** IHC (left) and quantification (right) of OLIG2 in mouse tumors from ish*CLOCK* and ishControl GSC272 models. Scale bar, 100 μm; $n = 3$ biological replicates; **, $P < 0.01$. **G,** IHC (left) and quantification (right) of Ki-67 in mouse tumors from ish*CLOCK* and ishControl GSC272 models. Scale bar, 100 μm; $n = 3$ biological replicates; **, $P < 0.01$. **H,** Immunofluorescence (left) and quantification (right) of microglia marker CX3CR1 in mouse tumors from ish*CLOCK* and ishControl GSC272 models. Scale bar, 100 μm; $n = 3$ biological replicates; **, $P < 0.01$. **I,** Kaplan–Meier survival curves of SCID mice implanted with GSC272 cells (5×10^5 cells) expressing shRNA control (shC) or *OLFML3* shRNAs ($n = 10$, 7, and 8 mice for shC, sh*OLFML3* #1 and sh*OLFML3* #3 groups, respectively). ***, $P < 0.001$.

LOX-expressing glioma cells and SPP1-expressing TAMs which support glioma cell survival (12). Thus, with respect to CSF1R inhibitors, it is tempting to speculate that patients with *PTEN*-deficient GBM may be particularly susceptible to such agents targeting TAMs. Along similar lines, our discovery here of the CLOCK–OLFML3–microglia axis and the correlative studies in human GBM TMAs showing high CLOCK and abundant microglia encourages the design of clinical trials targeting OLFML3 in patients with high-CLOCK GBM. We believe that targeting CLOCK–BMAL1 downstream targets,

Published OnlineFirst January 9, 2020; DOI: 10.1158/2159-8290.CD-19-0400

as opposed to CLOCK–BMAL1 directly, provides a superior therapeutic strategy given the likelihood of disturbed sleep cycles by targeting circadian regulators. Finally, microglia are well known to be immunosuppressive cells in the GBM TME and may therefore dampen immune checkpoint blockade activity (50); thus, it is tempting to speculate that combined inhibition of OLFML3 and immune checkpoint blockade may also prove beneficial for patients with GBM.

METHODS

Cell Culture

HMC3 microglia were cultured in Eagle's Minimum Essential Medium. CT2A, U87, and 293T cell lines were cultured in DMEM. All cell lines were cultured in the indicated medium containing 10% FBS (Sigma) and 1:100 antibiotic–antimycotic (Gibco), and were purchased from the ATCC. p53DN-hNSCs were generated by our laboratory as described recently (26). Patient-derived GSCs were provided by Dr. Erik P. Sulman and Dr. Frederick F. Lang from the Brain Tumor Center (The University of Texas MD Anderson Cancer Center). Mouse 005 and QPP7 GSCs were provided by Dr. Samuel D. Rabkin (Massachusetts General Hospital, Harvard Medical School) and Dr. Jian Hu (The University of Texas MD Anderson Cancer Center). All GSCs and neural stem cells (NSC) were cultured in NSC proliferation medium (Millipore Corporation) containing 20 ng/mL EGF and 20 ng/mL basic fibroblast growth factor. These GSCs and NSCs have been validated through fingerprinting by the MD Anderson Cell Line Core Facility. All cells were confirmed to be *Mycoplasma*-free, and maintained at 37°C and 5% CO_2. CM were collected from treated or untreated cells as indicated after culturing for 24 hours in FBS-free culture medium.

Tumorsphere Formation Assay

Soft-agar colony formation assay and tumorsphere formation were performed as described previously (51).

Epigenetic Screen

The open reading frame (ORF) lentiviral vectors in the Precision LentiORF collection were obtained from the Functional Genomics Facility at MD Anderson Cancer Center. In 96-well plates, we packaged 284 ORF lentiviruses (encoding known epigenetic factors) individually and infected with p53DN-hNSCs. Stable sublines were generated by blasticidin selection and then subjected to soft-agar colony formation assay.

Plasmids, Viral Transfections, and Cloning

shRNAs targeting human and mouse *CLOCK*, *BMAL1*, and *OLFML3* in the pLKO.1 vector (Sigma) were used in this study. Lentiviral particles (8 μg) were generated by transfecting 293T cells with the packaging vectors psPAX2 (4 μg) and pMD2.G (2 μg). Lentiviral particles were collected 48 and 72 hours after transfection of 293T cells, filtered through a 0.45-μm filter (Corning), and then used to treat cells in culture. After 48 hours, cells were selected by puromycin (2 μg/mL). The following human shRNA sequences (*CLOCK*: #74: TRCN0000018974 and #75: TRCN0000018975; *BMAL1*: #96: TRCN0000019096 and #98: TRCN0000019098; and *OLFML3*: #1: TRCN0000186745 and #3: TRCN0000203502) and mouse shRNA sequences (*Clock*: #1:TRCN0000095686 and #2 TRCN0000306474; *Bmal1*: #54: TRCN0000095054 and #57: TRCN0000095057) were selected for further use following the validation. Doxycycline-inducible plasmids were generated by cloning the desired shRNA sequences (sh*CLOCK* #75) into a pLKO.1 vector through the Gateway Cloning System (Thermo Fisher Scientific). Following transfection, cells were treated with doxycycline (2 μg/mL) for 48 hours to knock down *CLOCK*. For rescue experiments, *CLOCK* shRNA knockdown QPP7 cells were transfected with a human *CLOCK* construct that is resistant to *CLOCK* shRNAs (sh*CLOCK* #1 and #2).

Immunoblotting

Immunoblotting was performed following standard protocol (12). Antibodies were purchased from the indicated companies, including antibodies against β-actin (Sigma, #A3854), vinculin (EMD Millipore, #05-386), CLOCK (Cell Signaling Technology, #5157S), BMAL1 (Cell Signaling Technology, #14020S), and OLFML3 (Invitrogen, #PA5-31581).

IHC and Immunofluorescence

IHC was performed as standard protocol. In brief, a pressure cooker (95°C for 30 minutes followed by 120°C for 10 seconds) was used for antigen retrieval using antigen unmasking solution (Vector Laboratories). Antibodies specific to CLOCK (Cell Signaling Technology, #5157S), BMAL1 (Cell Signaling Technology, #14020S), CX3CR1 (Invitrogen, #702321), TMEM119 (BioLegend, #853302), CD206 (R&D Systems, #AF2535), cleaved caspase-3 (Cell Signaling Technology, #9661S), OLIG2 (Millipore, #AB15328), nestin (Millipore, #MAB5326), and Ki-67 (Thermo Fisher Scientific, #RM-9106-S1) were used in this study. The human and mouse tumor tissue sections were reviewed and scored by TMARKER software (52). Slides were scanned using Pannoramic 250 Flash III (3DHISTECH Ltd) and images were captured through Pannoramic Viewer software (3DHISTECH Ltd). The studies related to human specimens were approved by the MD Anderson Institutional Review Board under protocol #PA14-0420. Immunofluorescence was performed as described previously (12), and antibodies specific to CX3CR1 (Invitrogen, #702321) were used. Images were captured using a fluorescence microscope (Leica DMi8).

Migration Assay

Human microglia HMC3 cells (5×10^5) were suspended in serum-free culture medium and seeded into 24-well Transwell inserts (8 μm). Medium with indicated factors or CM was added to the remaining receiver wells. After 24 hours, the migrated microglia were fixed and stained with crystal violet (0.05%, Sigma) and then counted as cells per field of view under microscope.

ChIP-PCR and Luciferase Reporter Assay

ChIP-PCR was performed using the standard protocol. Briefly, GSC272 cells were cross-linked using 1% paraformaldehyde (PFA; 10 minutes) and then reactions were quenched using glycine (5 minutes) at room temperature. Cells were lysed with ChIP lysis buffer for 30 minutes on ice. Chromatin fragmentation was performed using a Diagenode Bioruptor Pico sonicator (45 cycles, each with 30 seconds on and 30 seconds off). Solubilized chromatin was then incubated with a mixture of antibody [CLOCK (Abcam, #ab3517) or BMAL1 (Cell Signaling Technology, #14020S)] and Dynabeads (Life Technologies) overnight. Immune complexes were then washed with RIPA buffer three times, once with RIPA-500 and once with LiCl wash buffer. Elution and reverse cross-linking were performed in direct elution buffer containing proteinase K (20 mg/mL) at 65°C overnight. Eluted DNA was purified using AMPure beads (Beckman-Coulter), and then was used to perform qPCR. The *OLFML3* primer was designed according to the E-box of human *OLFML3* gene (−412 to −229 bp; forward: TGACCACTTGGGCCATTGTT; reverse: CAGCAAACGCCATTCCT GTT). To perform the luciferase reporter assay, the promoter region of human *OLFML3* (−412 to −229 bp to ATG) was amplified by PCR and inserted into the *Bgl*II/*Hin*dIII sites of the pGL3 vector to generate the corresponding reporter constructs with or without point mutations in human *OLFML3* E-box sites. The luciferase reporter assay was conducted by transfecting the reporter constructs, *CLOCK* expression vector, and *Renilla* luciferase vector into 293T cells. Cells were harvested after 24 hours of transfection and luciferase activities were measured.

Quantitative Real-Time PCR

Cells were pelleted and RNA was isolated with the RNeasy Mini Kit (Qiagen). RNA was reverse-transcribed into cDNA by following

Published OnlineFirst January 9, 2020; DOI: 10.1158/2159-8290.CD-19-0400

the ABM cDNA Synthesis Kit. Quantitative real-time PCR (qRT-PCR) was performed using SYBR Green PCR Master Mix (Thermo Fisher Scientific) in a 7500 Fast Real-Time PCR Machine (Applied Biosystems). qRT-PCR primers are listed in Supplementary Table S1. The expression of each gene was normalized to that of *GAPDH*.

Microarray Analysis

RNA was isolated as described above with slight modifications. ishControl and ish*CLOCK* GSC272 cells ($n = 2$ biological replicates) were first lysed with Buffer RLT, then purified with TRIzol Reagent (Life Technologies) and chloroform. The remaining steps of the RNeasy Mini Kit were then followed. Microarray experiments were conducted by the MD Anderson Sequencing and Microarray Core Facility using the Clariom D Assay (Thermo Fisher Scientific). Microarray experiments were performed in duplicate. The raw data were processed and analyzed by GenePattern using Transcriptome Analysis Console. Genes that were differentially expressed between ishControl and ish*CLOCK* GSC272 were subjected to GSEA.

Mice and Intracranial Xenograft Tumor Models

Female ICR SCID mice (3–4 weeks age) were purchased from Taconic Biosciences. Mice were grouped by 5 animals in large plastic cages and were maintained under pathogen-free conditions. All animal experiments were performed with the approval of MD Anderson Cancer Center's Institutional Animal Care and Use Committee. The intracranial xenograft tumor model in SCID mice was established as we described recently (26). The mice were bolted and intracranially implanted with cells at MD Anderson's Brain Tumor Center Animal Core. Mice with neurologic deficits or moribund appearance were sacrificed, and the tumor tissues were harvested for histologic analysis. Following transcranial perfusion with 4% PFA, brains were removed and fixed in formalin, and were processed for paraffin-embedded blocks.

Human Samples

Tissue microarrays containing 35 human GBM samples and 5 normal brain tissues were purchased from US Biomax (catalog no. GL806f).

Computational Analysis of Human GBM Data

For analysis of human GBM data, we downloaded the gene-expression and copy-number data of TCGA datasets or other available datasets from GlioVis: http://gliovis.bioinfo.cnio.es/ or cBioPortal: https://www.cbioportal.org/. The expression and correlation of interesting genes in GBM, and GOEA were analyzed using GlioVis.

Statistical Analysis

All statistical analyses were performed with Student *t* test and represented as mean ± SD unless noted otherwise. The analysis of GBM TCGA database and TAM IHC staining for the correlation between genes or proteins was performed using the Pearson Correlation test (GraphPad Prism 7). The analysis of the survival data from the GBM TCGA database was performed using the Log-rank (Mantel-Cox) test (GraphPad Prism 7). The *P* values were designated as *, $P < 0.05$; **, $P < 0.01$; ***, $P < 0.001$; and n.s., nonsignificant ($P > 0.05$).

Data and Software Availability

The newly generated microarray data have been submitted to the Gene Expression Omnibus repository, and the accession number is GSE140409.

Disclosure of Potential Conflicts of Interest

Y.A. Wang is a consultant for Merck, the Department of Defense, and the Emerson Collective. R.A. DePinho is a co-founder, advisor, and director at Tvardi Therapeutics. No potential conflicts of interest were disclosed by the other authors.

Authors' Contributions

Conception and design: P. Chen, W.-H. Hsu, Z. Tan, Y.A. Wang, R.A. DePinho
Development of methodology: P. Chen, W.-H. Hsu, Z. Tan, Y.A. Wang
Acquisition of data (provided animals, acquired and managed patients, provided facilities, etc.): P. Chen, W.-H. Hsu, A. Chang, Z. Lan, A. Zhou, F.F. Lang, Y.A. Wang, R.A. DePinho
Analysis and interpretation of data (e.g., statistical analysis, biostatistics, computational analysis): P. Chen, W.-H. Hsu, A. Chang, A. Zhou, Y.A. Wang
Writing, review, and/or revision of the manuscript: P. Chen, A. Chang, D.J. Spring, Y.A. Wang, R.A. DePinho
Administrative, technical, or material support (i.e., reporting or organizing data, constructing databases): P. Chen, D.J. Spring, Y.A. Wang
Study supervision: P. Chen, Y.A. Wang, R.A. DePinho

Acknowledgments

This work was supported by the Cancer Research Institute Irvington Postdoctoral Fellowship (to P. Chen), The Harold C. and Mary L. Daily Endowment Fellowship (to P. Chen), the Caroline Ross Endowed Fellowship (to P. Chen), the Emerson Collective Award (to Y.A. Wang), NIH R01 CA231349 (to Y.A. Wang), the Clayton & Modesta William Cancer Research Fund (to R.A. DePinho), NIH P01 CA117969 (to R.A. DePinho), NIH R01 CA084628 (to R.A. DePinho), and the Burkhart III Distinguished University Chair in Cancer Research Endowment (to R.A. DePinho). The authors thank Dr. Michael D. Peoples for providing shRNAs, Dr. Erik P. Sulman for providing human-derived GSCs, and Drs. Samuel D. Rabkin and Jian Hu for providing mouse GSCs.

The costs of publication of this article were defrayed in part by the payment of page charges. This article must therefore be hereby marked *advertisement* in accordance with 18 U.S.C. Section 1734 solely to indicate this fact.

Received April 1, 2019; revised November 26, 2019; accepted January 6, 2020; published first January 9, 2020.

REFERENCES

1. Khosla D. Concurrent therapy to enhance radiotherapeutic outcomes in glioblastoma. Ann Transl Med 2016;4:54.
2. Zheng H, Ying H, Yan H, Kimmelman AC, Hiller DJ, Chen AJ, et al. Pten and p53 converge on c-Myc to control differentiation, self-renewal, and transformation of normal and neoplastic stem cells in glioblastoma. Cold Spring Harb Symp Quant Biol 2008;73:427–37.
3. Dunn GP, Rinne ML, Wykosky J, Genovese G, Quayle SN, Dunn IF, et al. Emerging insights into the molecular and cellular basis of glioblastoma. Genes Dev 2012;26:756–84.
4. Cancer Genome Atlas Research Network. Comprehensive genomic characterization defines human glioblastoma genes and core pathways. Nature 2008;455:1061–8.
5. Brennan CW, Verhaak RG, McKenna A, Campos B, Noushmehr H, Salama SR, et al. The somatic genomic landscape of glioblastoma. Cell 2013;155:462–77.
6. Stupp R, Mason WP, van den Bent MJ, Weller M, Fisher B, Taphoorn MJ, et al. Radiotherapy plus concomitant and adjuvant temozolomide for glioblastoma. N Engl J Med 2005;352:987–96.
7. McNamara MG, Lwin Z, Jiang H, Chung C, Millar BA, Sahgal A, et al. Conditional probability of survival and post-progression survival in patients with glioblastoma in the temozolomide treatment era. J Neurooncol 2014;117:153–60.
8. Li X, Wu C, Chen N, Gu H, Yen A, Cao L, et al. PI3K/Akt/mTOR signaling pathway and targeted therapy for glioblastoma. Oncotarget 2016;7:33440–50.
9. Westphal M, Maire CL, Lamszus K. EGFR as a target for glioblastoma treatment: an unfulfilled promise. CNS Drugs 2017;31:723–35.

Published OnlineFirst January 9, 2020; DOI: 10.1158/2159-8290.CD-19-0400

10. Wang G, Lu X, Dey P, Deng P, Wu CC, Jiang S, et al. Targeting YAP-dependent MDSC infiltration impairs tumor progression. Cancer Discov 2016;6:80–95.
11. Liao W, Overman MJ, Boutin AT, Shang X, Zhao D, Dey P, et al. KRAS-IRF2 axis drives immune suppression and immune therapy resistance in colorectal cancer. Cancer Cell 2019;35:559–72.
12. Chen P, Zhao D, Li J, Liang X, Li J, Chang A, et al. Symbiotic macrophage-glioma cell interactions reveal synthetic lethality in PTEN-null glioma. Cancer Cell 2019;35:868–84.
13. Romani M, Pistillo MP, Banelli B. Epigenetic targeting of glioblastoma. Front Oncol 2018;8:448.
14. Nagarajan RP, Costello JF. Epigenetic mechanisms in glioblastoma multiforme. Semin Cancer Biol 2009;19:188–97.
15. Kondo Y, Katsushima K, Ohka F, Natsume A, Shinjo K. Epigenetic dysregulation in glioma. Cancer Sci 2014;105:363–9.
16. Gimple RC, Bhargava S, Dixit D, Rich JN. Glioblastoma stem cells: lessons from the tumor hierarchy in a lethal cancer. Genes Dev 2019;33:591–609.
17. Yelton CJ, Ray SK. Histone deacetylase enzymes and selective histone deacetylase inhibitors for antitumor effects and enhancement of antitumor immunity in glioblastoma. Neuroimmunol Neuroinflamm 2018;5:46.
18. Miranda A, Hamilton PT, Zhang AW, Pattnaik S, Becht E, Mezheyeuski A, et al. Cancer stemness, intratumoral heterogeneity, and immune response across cancers. Proc Natl Acad Sci U S A 2019;116:9020–9.
19. Sulli G, Lam MTY, Panda S. Interplay between circadian clock and cancer: new frontiers for cancer treatment. Trends Cancer 2019;5:475–94.
20. Masri S, Sassone-Corsi P. The emerging link between cancer, metabolism, and circadian rhythms. Nat Med 2018;24:1795–803.
21. Shafi AA, Knudsen KE. Cancer and the circadian clock. Cancer Res 2019;79:3806–14.
22. Buhr ED, Takahashi JS. Molecular components of the mammalian circadian clock. Handb Exp Pharmacol 2013;217:3–27.
23. Puram RV, Kowalczyk MS, de Boer CG, Schneider RK, Miller PG, McConkey M, et al. Core circadian clock genes regulate leukemia stem cells in AML. Cell 2016;165:303–16.
24. Li A, Lin X, Tan X, Yin B, Han W, Zhao J, et al. Circadian gene Clock contributes to cell proliferation and migration of glioma and is directly regulated by tumor-suppressive miR-124. FEBS Lett 2013;587:2455–60.
25. Dong Z, Zhang G, Qu M, Gimple RC, Wu Q, Qiu Z, et al. Targeting glioblastoma stem cells through disruption of the circadian clock. Cancer Discov 2019;9:1556–73.
26. Hu B, Wang Q, Wang YA, Hua S, Sauve CG, Ong D, et al. Epigenetic activation of WNT5A drives glioblastoma stem cell differentiation and invasive growth. Cell 2016;167:1281–95.
27. Schibler U, Gotic I, Saini C, Gos P, Curie T, Emmenegger Y, et al. Clock-talk: interactions between central and peripheral circadian oscillators in mammals. Cold Spring Harb Symp Quant Biol 2015;80:223–32.
28. Sulli G, Rommel A, Wang XJ, Kolar MJ, Puca F, Saghatelian A, et al. Pharmacological activation of REV-ERBs is lethal in cancer and oncogene-induced senescence. Nature 2018;553:351–5.
29. Engler JR, Robinson AE, Smirnov I, Hodgson JG, Berger MS, Gupta N, et al. Increased microglia/macrophage gene expression in a subset of adult and pediatric astrocytomas. PLoS One 2012;7:e43339.
30. Bindea G, Mlecnik B, Tosolini M, Kirilovsky A, Waldner M, Obenauf AC, et al. Spatiotemporal dynamics of intratumoral immune cells reveal the immune landscape in human cancer. Immunity 2013;39:782–95.
31. Bowman RL, Klemm F, Akkari L, Pyonteck SM, Sevenich L, Quail DF, et al. Macrophage ontogeny underlies differences in tumor-specific education in brain malignancies. Cell Rep 2016;17:2445–59.
32. Chen Y, Zhang Y, Yin Y, Gao G, Li S, Jiang Y, et al. SPD–a web-based secreted protein database. Nucleic Acids Res 2005;33(Database issue):D169–73.
33. Saha D, Martuza RL, Rabkin SD. Macrophage polarization contributes to glioblastoma eradication by combination immunovirotherapy and immune checkpoint blockade. Cancer Cell 2017;32:253–67.
34. Hambardzumyan D, Gutmann DH, Kettenmann H. The role of microglia and macrophages in glioma maintenance and progression. Nat Neurosci 2016;19:20–7.
35. Kronauer RE, Gunzelmann G, Van Dongen HPA, Doyle FJ, Klerman EB. Uncovering physiologic mechanisms of circadian rhythms and sleep/wake regulation through mathematical modeling. J Biol Rhythm 2007;22:233–45.
36. Schernhammer ES, Laden F, Speizer FE, Willett WC, Hunter DJ, Kawachi I, et al. Night-shift work and risk of colorectal cancer in the nurses' health study. J Natl Cancer Inst 2003;95:825–8.
37. Fu L, Kettner NM. The circadian clock in cancer development and therapy. Prog Mol Biol Transl Sci 2013;119:221–82.
38. Quail DF, Joyce JA. Microenvironmental regulation of tumor progression and metastasis. Nat Med 2013;19:1423–37.
39. Matias D, Predes D, Niemeyer Filho P, Lopes MC, Abreu JG, Lima FRS, et al. Microglia-glioblastoma interactions: new role for Wnt signaling. Biochim Biophys Acta Rev Cancer 2017;1868:333–40.
40. Scheiermann C, Kunisaki Y, Frenette PS. Circadian control of the immune system. Nat Rev Immunol 2013;13:190–8.
41. Fonken LK, Kitt MM, Gaudet AD, Barrientos RM, Watkins LR, Maier SF. Diminished circadian rhythms in hippocampal microglia may contribute to age-related neuroinflammatory sensitization. Neurobiol Aging 2016;47:102–12.
42. Fonken LK, Frank MG, Kitt MM, Barrientos RM, Watkins LR, Maier SF. Microglia inflammatory responses are controlled by an intrinsic circadian clock. Brain Behav Immun 2015;45:171–9.
43. de Assis LVM, Kinker GS, Moraes MN, Markus RP, Fernandes PA, Castrucci AML. Expression of the circadian clock gene BMAL1 positively correlates with antitumor immunity and patient survival in metastatic melanoma. Front Oncol 2018;8:185.
44. He WY, Holtkamp S, Hergenhan SM, Kraus K, de Juan A, Weber J, et al. Circadian expression of migratory factors establishes lineage-specific signatures that guide the homing of leukocyte subsets to tissues. Immunity 2018;49:1175–90.e7.
45. Miljkovic-Licina M, Hammel P, Garrido-Urbani S, Lee BP, Meguenani M, Chaabane C, et al. Targeting olfactomedin-like 3 inhibits tumor growth by impairing angiogenesis and pericyte coverage. Mol Cancer Ther 2012;11:2588–99.
46. Neidert N, von Ehr A, Zoller T, Spittau B. Microglia-specific expression of Olfml3 is directly regulated by transforming growth factor beta 1-induced smad2 signaling. Front Immunol 2018;9:1728.
47. Quail DF, Bowman RL, Akkari L, Quick ML, Schuhmacher AJ, Huse JT, et al. The tumor microenvironment underlies acquired resistance to CSF-1R inhibition in gliomas. Science 2016;352:aad3018.
48. Pyonteck SM, Akkari L, Schuhmacher AJ, Bowman RL, Sevenich L, Quail DF, et al. CSF-1R inhibition alters macrophage polarization and blocks glioma progression. Nat Med 2013;19:1264–72.
49. Butowski N, Colman H, De Groot JF, Omuro AM, Nayak L, Wen PY, et al. Orally administered colony stimulating factor 1 receptor inhibitor PLX3397 in recurrent glioblastoma: an Ivy Foundation Early Phase Clinical Trials Consortium phase II study. Neuro-oncol 2016;18:557–64.
50. See AP, Parker JJ, Waziri A. The role of regulatory T cells and microglia in glioblastoma-associated immunosuppression. J Neurooncol 2015;123:405–12.
51. Ong DST, Hu B, Ho YW, Sauve CG, Bristow CA, Wang Q, et al. PAF promotes stemness and radioresistance of glioma stem cells. Proc Natl Acad Sci U S A 2017;114:E9086–E95.
52. Schuffler PJ, Fuchs TJ, Ong CS, Wild PJ, Rupp NJ, Buhmann JM. TMARKER: a free software toolkit for histopathological cell counting and staining estimation. J Pathol Inform 2013;4(Suppl):S2.

Published OnlineFirst January 9, 2020; DOI: 10.1158/2159-8290.CD-19-0400

AACR American Association for Cancer Research

CANCER DISCOVERY

Circadian Regulator CLOCK Recruits Immune-Suppressive Microglia into the GBM Tumor Microenvironment

Peiwen Chen, Wen-Hao Hsu, Andrew Chang, et al.

Cancer Discov Published OnlineFirst January 9, 2020.